

Doi: <http://dx.doi.org/10.1590/1809-4430-Eng.Agric.v41n2p255-262/2021>**TECHNICAL PAPER****SPATIAL AUTOCORRELATION OF PHYSICAL ATTRIBUTES OF AN OXISOL****Job T. de Oliveira^{1*}, Rubens A. de Oliveira¹,
Fernando F. da Cunha¹, Eduardo S. dos Santos²**

^{1*}Corresponding author. Universidade Federal do Mato Grosso do Sul (UFMS), Câmpus de Chapadão do Sul/ Chapadão do Sul - MS, Brasil. E-mail: job.oliveira@hotmail.com | ORCID ID: <https://orcid.org/0000-0001-9046-0382>

KEYWORDS

precision agriculture, spatial dependence, geostatistics, Moran index.

ABSTRACT

Studies that seek to identify a smaller number of soil attributes that represent others can generate less expenditure of time and financial resources for monitoring cultivated areas. Thus, this study aimed to analyze the spatial distribution and spatial autocorrelation of physical attributes of an Oxisol (Latossolo Vermelho Amarelo, Brazilian Soil Classification System). The evaluated attributes consisted of soil density (SD), total porosity (TP), free porosity (FP), field capacity (FC), permanent wilt point (PW), and total water availability (TW). Semivariogram adjustments and semivariance estimates were performed to characterize the structure and magnitude of the spatial dependence of soil attributes. The attributes were distributed on thematic maps and the spatial autocorrelation was estimated by the Moran index, which quantifies the degree of autocorrelation. TP showed a high positive correlation with PWP. Soil TW showed a high positive correlation with SD and a high negative correlation with FP. In turn, FP showed a high negative correlation with SD. The results showed spatial dependence for all attributes, standing out the apparent soil density and permanent wilt point, which were good evaluators of strong spatial dependence.

INTRODUCTION

Changes in soil structure, evidenced by alterations in its density, affect different soil physico-hydric attributes (Tavanti et al., 2020). These attributes include total porosity, pore diameter distribution, aeration porosity, water storage and availability for plants, and water dynamics on the surface and in the soil profile. All these attributes are important but evaluating them all together is not a quick and cheap task. Thus, alternatives to overcome these problems should be sought. One possible way would be to evaluate a smaller number of attributes that represent the majority, i.e., verify which attributes have higher autocorrelations and estimate the others from them (Oliveira, 2020b).

Spatial autocorrelation can be defined as the coincidence of similar values in close locations or even the absence of randomness of a variable due to its spatial distribution (Neves et al., 2015). Two forms of spatial

autocorrelation can occur: a positive autocorrelation, when high or low values for a random variable tend to cluster in space, and a negative autocorrelation, when a dissimilarity is found in the data between the high and low values spatially distributed (Anselin et al., 2006; Neves et al., 2015).

Spatial autocorrelation can be measured in different ways, including the Moran index (I). I is a very widespread statistic and determines the spatial autocorrelation from the product of deviations from the mean. This index is a global measure of spatial autocorrelation, as it indicates the degree of the spatial association present in the data set. In general, the Moran index is used in a test whose null hypothesis represents spatial independence. In this case, its value would be zero. Positive values between 0 and +1 indicate a direct correlation, while negative values between 0 and -1 indicate an inverse correlation (Almeida, 2012).

The spatial correlation analysis can be performed using several tools. Georeferencing, spatial distribution, and the use of thematic maps in production fields are techniques

¹ Universidade Federal de Viçosa (UFV)/ Viçosa - MG, Brasil.

² Universidade Federal do Maranhão (UFMA)/ Chapadinha - MA, Brasil.

Area Editor: Fabio Henrique Rojo Baio

Received in: 5-27-2020

Accepted in: 12-14-2020



of great importance in the analysis of risks to crop management. The analysis of the spatial distribution of indicators is an instrument that can contribute to understanding the processes involved in a particular phenomenon to be studied, allowing the analysis of characteristics and differences of each territorial space beyond the simple geographical view, covering the constructed production space (Oliveira, 2020b).

Tavanti et al. (2020) highlighted the importance of studying the physical quality of soils, and these evaluations can be applied for studies of spatial variability of soil attributes and precision agriculture, thus assisting in decisions related to the physical management of soils.

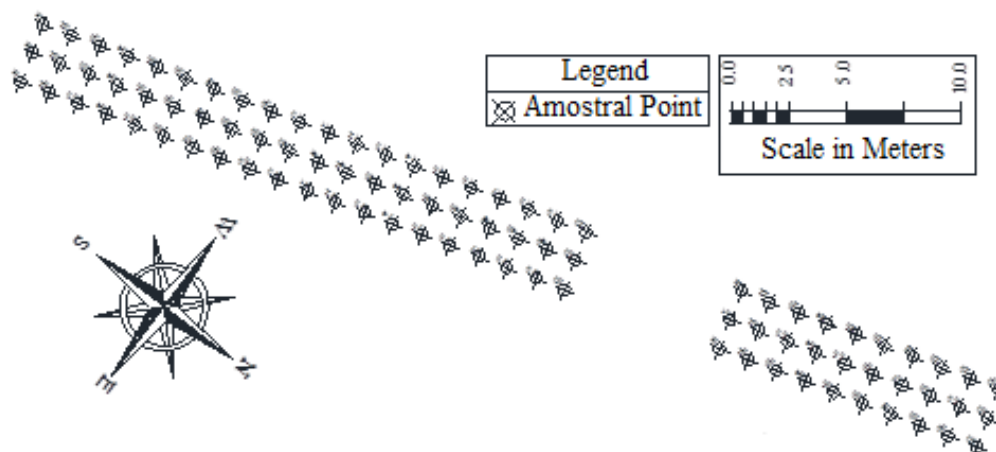


FIGURE 1. Sampling grid and details of the sampling carried out in the irrigation and drainage area of the Federal University of Viçosa, Viçosa, Minas Gerais, Brazil.

The average temperature in Viçosa is 20.6 °C and the climate is classified as Cwa according to the Köppen and Geiger classification. The average annual rainfall is 1229 mm, and its distribution is concentrated mainly in the summer period.

The soil in which the experimental grids were installed was classified as a sand clay-textured Oxisol (Latossolo Vermelho Amarelo, Brazilian Soil Classification System) according to EMBRAPA (2018). The particle size analysis in the layers of 0.0 to 0.2 m showed values of 460, 150, and 390 g kg⁻¹ for sand, silt, and clay, respectively. Soil chemical analysis showed average values of pH (in H₂O) of 6.0, organic matter content of 2.18 dag kg⁻¹, P and K of 21.2 and 135.0 mg dm⁻³, respectively, and sum of bases and CEC of 3.7 and 6.1 cmol_c dm⁻³, respectively.

The *x* and *y* directions of the Cartesian coordinate system were defined, and the experimental grid was staked in the second ten-day period of September 2018, spaced at 1.60 m from each other. The experimental grid represented an area of 230.4 m² and consisted of 90 sample points with dimensions of 1.60 × 1.60 m.

The experimental area has been explored for many years with successive crops, such as corn, bean, and passion fruit. The soil was cultivated with purple noble garlic of the variety Ito during the soil analysis period.

Laboratory analyses were carried out from October to November 2018. Soil samples with a preserved structure were taken to determine soil physical properties at depths of 0 to 0.10 m (1) and 0.10 to 0.20 m (2). A Kopecky steel ring with sharp edges and dimensions of 50 mm in height and 50 mm in diameter was used. The following soil physical

attributes represent others can generate less time and financial resources to monitor cultivated areas. Thus, this study aimed to analyze the spatial distribution and spatial autocorrelation of physical attributes of an Oxisol (Latossolo Vermelho Amarelo, Brazilian Soil Classification System).

MATERIAL AND METHODS

The study was carried out in the irrigation and drainage area at the Federal University of Viçosa, Viçosa, Minas Gerais, Brazil (Figure 1). This area is located close to the geographic coordinates: 23 K, 722569.09 m E; 7701897.59 m S (UTM).

attributes were obtained: apparent soil density (SD1 and SD2), which consisted of the relationship between the dry soil and its volume; total porosity (TP1 and TP2), consisting of determining the total pore volume of the soil occupied by water and/or air; free porosity (FP1 and FP2), which is the difference between the total porosity and volumetric soil moisture; field capacity (FC1 and FC2), which was obtained with a tension of 0.01 MPa, determined with the Richards extractor; permanent wilting point (PW1 and PW2), obtained with a tension of 1.5 MPa, determined with the Richards extractor; and total soil water availability (TW1 and TW2).

TWA was obtained according to [eq. (1)], being adapted from Bernardo et al. (2019). However, this equation is appropriate only to determine the amount of water in the 10 cm soil layer. The other soil physical attributes were obtained following the methodologies presented by EMBRAPA (2018).

$$TW = SD (FC - PW) \quad (1)$$

Where:

TW is the total soil water availability (mm);

SD is the soil density (g cm⁻³);

FC is the field capacity (% db), and

PW is the permanent wilt point (% db).

A classical descriptive analysis was performed for each studied attribute using the statistical program Rbio v. 17 (biometric in R). The mean, median, minimum, and

maximum values, standard deviation, coefficient of variation, data normality by Shapiro-Wilk method, and Pearson correlation, presented as a correlation network, were calculated.

The Moran index provides statistical significance and shows whether the data are randomly distributed. The results of Moran's bivariate correlation were expressed graphically by the correlation network, in which the proximity between nodes (features) was proportional to the absolute value between their correlation. The edge thickness was controlled by applying a cut-off value of 0.50, which meant that only $|r_{ij}| \geq 0.50$ had the edges highlighted. Finally, positive correlations were represented in green, while negative correlations were represented in red.

The structure and magnitude of spatial dependence on soil attributes were characterized by adjusting semivariograms and estimating the semivariance through the coefficients of the theoretical model for the semivariogram, that is, the nugget effect (C_0), sill (C_0+C), and the range (A_0).

The global Moran and local Moran (LISA) indices

were used as statistical tools for spatial autocorrelation. Spatial autocorrelation measures the relationship between observations with spatial proximity, considering that spatially close observations have similar values (Nascimento et al., 2007). The global indicators of spatial autocorrelation (Moran I and II) provide measurements for the set of all points of the geostatistical grid, characterizing the entire study region.

One possibility to visualize the global spatial autocorrelation is through Moran's scatter diagram (Figure 2). The variable of interest (X) is placed on the horizontal axis and the spatial lag of the variable of interest (W_X) is placed on the vertical axis. The diagram allows verifying the pattern of data concentration divided into four types of associations: high-high (HH), low-low (LL), low-high (LH), and high-low (HL). The regression line is increasing and the values of soil attributes tend to group in the first and third quadrants in case of positive spatial association, and the regression line is decreasing and units are predominantly grouped in the second and fourth quadrants when the relationship is negative (Almeida, 2012).

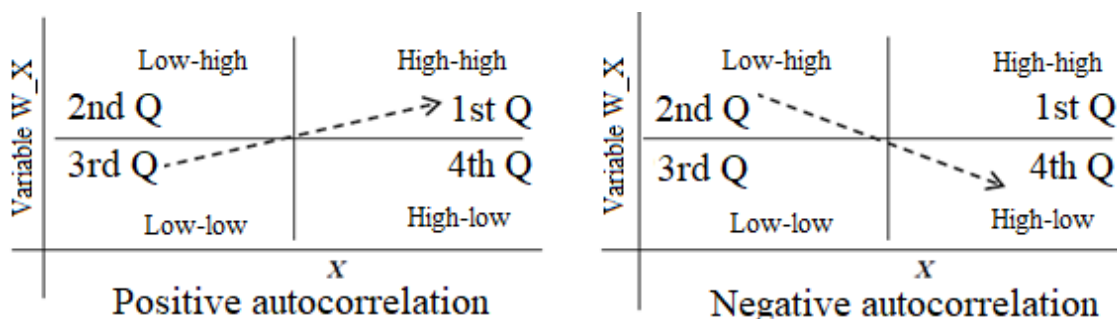


FIGURE 2. Moran's scatter diagram. Adapted from Almeida (2012).

The 5% significance level ($p < 0.05$) was considered in the analyses and the cartographic products were elaborated using the software QGIS 3.6.0. The pseudo-significance level of Moran's bivariate index was tested by the software GeoDa, using randomization with the processing of 999 permutations. These permutations are used to perform a statistical pseudo-test based on the Monte Carlo method (Anselin et al., 2006).

RESULTS AND DISCUSSION

The data from the descriptive analysis of soil attributes are shown in Table 1. The analysis of the minimum, maximum, and mean values and the variance of attribute values showed a considerable variation in the data. However, the knowledge of this variation alone is not sufficient to identify the locations where the high and low values of an attribute are found.

TABLE 1. Descriptive statistics of soil attributes.

Attribute ^(a)	Mean	Minimum	Maximum	Standard deviation	Coefficient of variation (%)	Pr<w	FD
SD1	1.15	1.00	1.30	0.08	7.06	1.3×10^{-7}	ID
TP1	47.42	33.90	56.80	4.01	8.45	0.0759	NO
FP1	20.23	10.80	39.00	6.01	29.74	0.0054	ID
FC1	31.72	27.30	36.60	1.85	5.82	0.5250	NO
PW1	17.09	15.70	18.60	0.54	3.18	0.9235	NO
TW1	50.72	36.70	71.00	7.16	14.12	0.2154	NO
SD2	1.12	0.90	1.30	0.08	7.41	4.5×10^{-7}	ID
TP2	49.29	34.40	72.10	5.38	10.92	1.9×10^{-7}	ID
FP2	20.68	10.00	51.50	7.90	38.18	5.6×10^{-5}	ID
FC2	32.79	25.70	39.20	1.88	5.73	6.3×10^{-4}	ID
PW2	17.52	16.10	19.10	0.62	3.52	0.7420	NO
TW2	51.11	26.20	62.90	6.09	11.92	0.0042	ID

SD = soil density ($g\ cm^{-3}$); TP = total porosity (%); FP = free porosity (%); FC = field capacity (%); PW = permanent wilting point (%); TW = total water availability (mm); FD = frequency distribution: NO, normal frequency distribution and ID, indeterminate frequency distribution. Pr<w = probability of the Shapiro-Wilk test at the 5% probability level.

Table 1 shows the descriptive analysis of the studied attributes. Oliveira et al. (2020a) observed that the variability of an attribute can be classified according to the magnitude of its coefficient of variation (CV). The classes were determined as low ($CV < 10\%$), medium ($10\% < CV < 20\%$), high ($20\% < CV < 30\%$), and very high ($CV > 30\%$). Therefore, the attributes varied from low to very high, with SD1, TP1, FC1, PW1, SD2, FC2, and PW2 showing low variability. The attributes TW1 and TP2 showed a medium coefficient of variation. Martins et al. (2019) studied the effects of spatial variability of soil attributes and found low and medium coefficients of variation for SD, with values of 9.12 and 10.80%, respectively. Soares et al. (2018) found low coefficients of variation for SD and TP. The variability rates from low to

very high found for soil attributes can possibly be explained by the fact that the studied soil is heterogeneous, de-standardizing the coefficient of variation of the studied attributes.

The correlation network of Moran's bivariate analyses (Figure 3) showed negative and significant correlations between SD1 and TP1, TP1 and TW1, FP1 and TW1, TP2 and SD2, with values of correlation coefficients of -0.1869^{**} , -0.1751^{**} , -0.1973^{**} , and -0.1597^{**} , respectively. These results were already expected. SD is the denominator of a fraction that is subtracted by the unit to calculate TP and hence the lower the SD, the higher the TP. Oliveira et al. (2020b) correlated physical attributes and highlighted the importance of maintaining good soil porosity conditions.

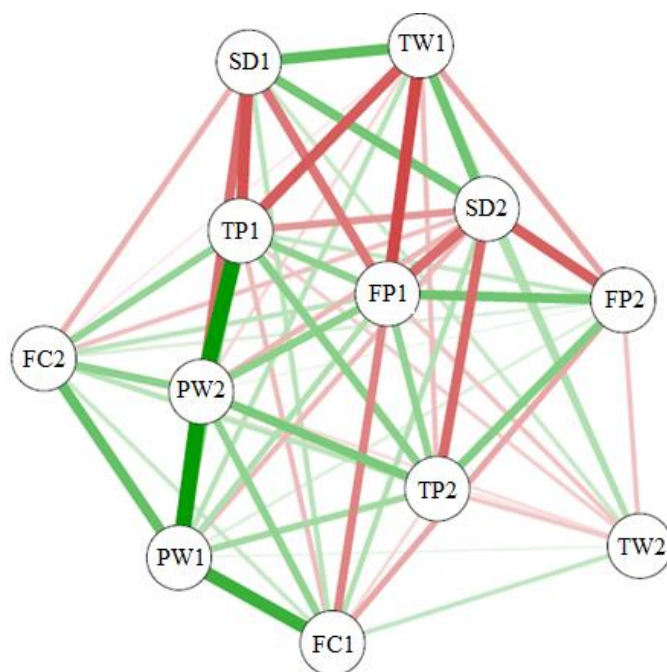


FIGURE 3. Correlation network of Moran's bivariate analysis of the attributes soil density (SD, g cm^{-3}), total porosity (TP, %), free porosity (FP, %), field capacity (FC, %), permanent wilting point (PW, %), and total water availability (TW, mm). Green lines represent positive correlation and red lines represent negative correlations. Line thickness indicates the highest degree of correlation.

Regarding TP and TW, we can initially imagine that the higher the volume of empty spaces, the higher the amount of water that the soil can store and, consequently, the higher the TW. It would be valid when comparing different soils, but the soil is the same in this research. Therefore, this difference in TP may have been caused by compaction processes and, thus, soil macroporosity may have been reduced to a higher extent than microporosity. Water is retained in soil micropores and, consequently, the volume occupied by macropores may have been replaced by another volume occupied with soil particles and microporosity, thus increasing soil water retention. It can be confirmed by the negative correlation between FP and TW. Tavanti et al. (2020) found negative correlations between soil quality and the water available in the soil.

Significant positive correlations were observed between the attributes TW1 and SD1, PW1 and FC1, PW2 and PW1, and FC2 and PW2, with values of 0.1752^{**} , 0.2120^{**} , 0.2708^{**} , and 0.1239^{**} , respectively. The positive correlation between TW and SD also corroborates with the explanation for TP and TW. Imagine scenario 1 in

which we have a volume occupied by soil particles (macro- and microporosity). If we use more soil to fill that same volume, we will have scenario 2, in which macropores will be reduced to make room for this new soil to be inserted. Thus, we will have a higher mass for the same volume and, consequently, higher SD. On the other hand, assuming that most of the microporosity was maintained from scenario 1 to 2 and more soil particle and microporosity entered scenario 2, we may conclude that scenario 2 will have higher microporosity and, consequently, higher water retention, affecting TW.

Several studies in the literature have corroborated the positive correlation between FC and PW (Alencar et al., 2009; Bezerra et al., 2019). Some methodologies in the literature can be used to estimate PW from FC, confirming this high positive correlation.

The geostatistical analysis (Table 2) showed spatial dependence for all the studied attributes. Cross-semivariograms adjusted to the spherical and Gaussian models. Oliveira et al. (2020a) also found the same adjustment models in a study performed with soil physical attributes.

TABLE 2. Parameters estimated for simple and cross-semivariograms of soil physical attributes.

Attribute ^(a)	Model ^(b)	Nugget effect (Co)	Sill (Co+C)	Range (Ao, m)	r ²	SSR ^(c)	SDE ^(d)	
							%	Class
Simple semivariogram								
SD1	exp	9.40x10 ⁻⁴	0.01	4.5	0.522	2.97x10 ⁻⁶	0.831	Strong
TP1	exp	4.91	1.64x10 ¹	4.0	0.522	1.89x10 ¹	0.700	Moderate
FP1	gau	1.37x10 ¹	3.75x10 ¹	3.5	0.762	4.27x10 ¹	0.635	Moderate
FC1	exp	2.30	3.60	16.0	0.441	0.77	0.361	Moderate
PW1	exp	0.08	0.31	5.5	0.494	3.07x10 ⁻³	0.754	Strong
TW1	sph	2.32x10 ¹	5.05x10 ¹	3.0	0.537	9.03x10 ¹	0.540	Moderate
SD2	exp	1.20x10 ⁻³	0.01	7.0	0.433	3.16x10 ⁻⁶	0.783	Strong
TP2	sph	1.56x10 ¹	3.40x10 ¹	10.8	0.728	7.75x10 ¹	0.541	Moderate
FP2	sph	3.74x10 ¹	7.48x10 ¹	15.8	0.877	1.40x10 ²	0.500	Moderate
FC2	exp	1.84	3.70	13.0	0.377	0.84	0.503	Moderate
PW2	exp	0.08	0.31	7.0	0.474	3.9x10 ⁻³	0.761	Strong
TW2	exp	7.00	3.00x10 ¹	6.0	0.179	8.88x10 ¹	0.767	Strong
Cross-semivariogram								
TW1=f(SD1)	sph	0.03	0.31	4.9	0.740	8.02x10 ⁻³	0.89	Strong
PW1=f(FC1)	sph	0.00	0.40	4.9	0.936	3.31x10 ⁻³	1.00	Strong
PW2=f(PW1)	gau	0.03	0.26	5.1	0.959	1.30x10 ⁻³	0.88	Strong
FC2=f(PW2)	sph	0.22	0.50	11.2	0.813	1.41x10 ⁻²	0.57	Moderate
SD1=f(TP1)	sph	-0.03	-0.18	4.6	0.714	2.21x10 ⁻³	0.81	Strong
TP1=f(TW1)	gau	-4.28	1.41x10 ¹	4.5	0.788	1.17x10 ¹	0.70	Moderate
FP1=f(TW1)	gau	-0.01	1.02x10 ¹	4.7	0.703	3.41x10 ¹	1.00	Strong
TP2=f(SD2)	sph	-0.12	-0.27	10.9	0.885	2.00x10 ⁻³	0.55	Moderate

(a) SD = soil density (g cm⁻³); TP = total porosity (%); FP = free porosity (%); FC = field capacity (%); PW = permanent wilt point (%); TW = total water availability (mm). (b) sph = spherical; exp = exponential; and Gau = Gaussian. (c) SSR = sum of squared residuals. (d) SDE = spatial dependence evaluator.

A strong spatial dependence evaluator (SDE) occurs when semivariograms have a nugget effect < 25% of the sill, moderate when it is between 25 and 75%, and weak > 75%. According to this classification, which was used by Oliveira et al. (2020a, 2020b), the values of the variables SD1, PW1, SD2, PW2, and TW2, TW1=f(SD1), PW1=f(FC1), PW2=f(PW1), SD1=f(TP1), and FP1=f(TW1), presented a strong SDE.

The cross-semivariograms TW1=f(SD1), PW1=f(FC1), PW2=f(PW1), and FC2=f(PW2) showed a positive spatial dependence between variables, and

SD1=f(TP1), TP1=f(TW1), FP1=f(TW1), TP2=f(SD2) showed a negative spatial dependence between variables, as can be observed by the negative sign of the nugget effect and sill. The explanations for these behaviors would be the same as those already reported for the correlation network.

The use of Moran's bivariate index becomes an appropriate tool for determining spatial correlation. Figure 4 shows the significance maps of the soil attributes that present Moran's global bivariate indices verified in Figure 3 and cross-semivariograms in Table 2.

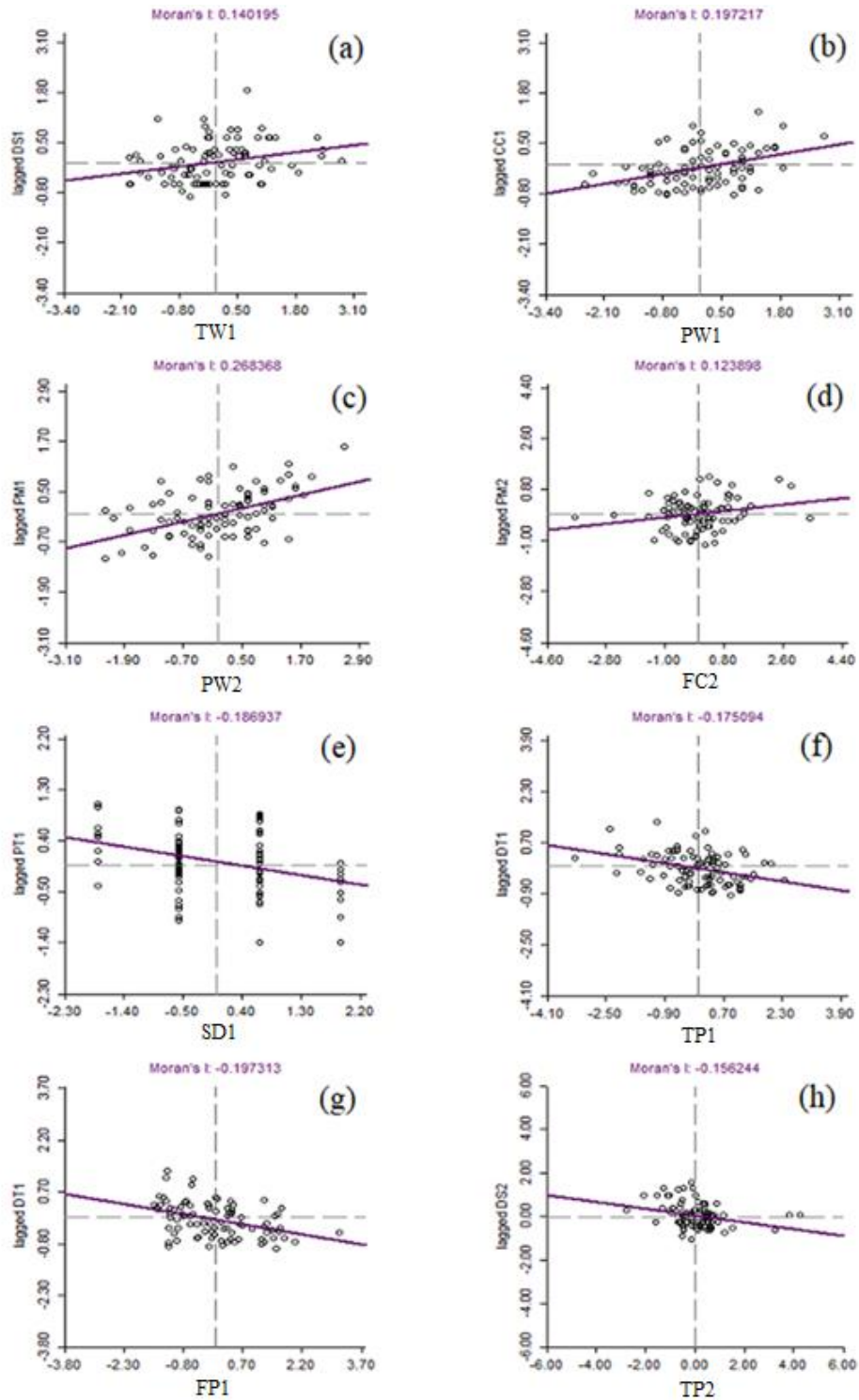


FIGURE 4. Moran's scatter diagram between (a) $TW1=f(SD1)$, (b) $PW1=f(FC1)$, (c) $PW2=f(PW1)$, (d) $FC2=f(PW2)$, (e) $SD1=f(TP1)$, (f) $TP1=f(TW1)$, (g) $FP1=f(TW1)$, and (h) $TP2=f(SD2)$. SD = soil density ($g\ cm^{-3}$); TP = total porosity (%); FP = free porosity (%); FC = field capacity (%); PW = permanent wilt point (%); TW = total water availability (mm).

Values were estimated using the cluster maps after adjusting the scatter diagrams (Figure 4) relative to soil attributes. In this sense, maps with concentration patterns were constructed for the studied variables (Figure 5), which showed the significant spatial clusters.

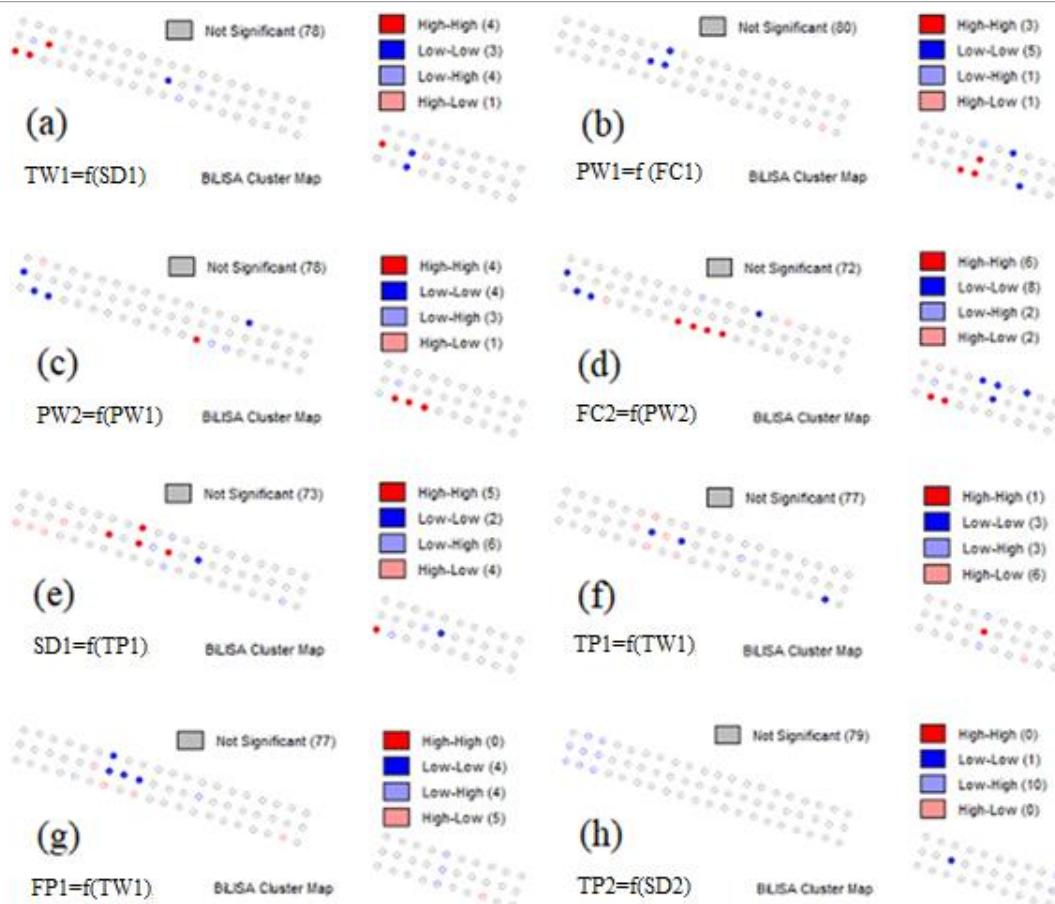


FIGURE 5. Cluster maps of Moran's bivariate indices: (a) $TW1=f(SD1)$, (b) $PW1=f(FC1)$, (c) $PW2=f(PW1)$, (d) $FC2=f(PW2)$, (e) $SD1=f(TP1)$, (f) $TP1=f(TW1)$, (g) $FP1=f(TW1)$, and (h) $TP2=f(SD2)$. SD = soil density ($g\ cm^{-3}$); TP = total porosity (%); FP = free porosity (%); FC = field capacity (%); PW = permanent wilt point (%); TW = total water availability (mm).

The maps of bivariate clusters (Figure 5) show which regions formed statistically significant spatial clusters at least 5% of the relationship between the soil attribute indicators. These mappings of bivariate regimes allow a more adequate geographic visualization of the degree of concentration of the studied variables, referring to the local bivariate Moran indices or local spatial autocorrelation analysis (Moran LISA).

Four statistically significant categories are shown. Regions in red represent clusters with a high concentration of the attribute under analysis. Locations in dark blue show the spatial associations with a low concentration of the attribute under analysis. Units highlighted in lighter blue and lighter red represent the atypical associations, that is, low-high and high-low, respectively.

The cluster map of total water availability as a function of soil density (Figure 5a) shows that 3.3% of the area (red dots), concentrated in the southern region, had similar results, that is, a high-high autocorrelation. A high-high clustering means that the spatial units present high values for the variable of interest, being surrounded by spatial units that also have high values.

The cluster map of the distribution of similar results of the high-high type between apparent wilt point and field capacity (Figure 5b) can be mostly observed in the northern

portion of the area, with 3.3% of the observations. The indication of these regions shows the similarities of higher values of soil wilt point and higher incidences of field capacities in the north of the experimental area.

The observation of these cluster maps together with field observations can contribute to finding the reasons for the occurrence of productivity variability of some crops of interest cultivated in the area. This identification allows the correction of possible failures, allowing minimizing problems in the next growing season.

The cluster map of free porosity as a function of total water availability (Figure 5g) shows that 4.4% of the area (blue dots) are concentrated in the southern portion and presented similar results, with a low-low autocorrelation. A low-low clustering refers to spatial units with low values surrounded by spatial units that also have low values.

Thus, the farmer can take advantage of the historical information of the area from mappings to make the necessary decisions to guide the correct crop management, identifying regions with a higher or lower need for intervention either in the soil or in the plant (Oliveira et al., 2018). This study can be a basis for irrigation management, soil management (fertility) at various rates, genetic improvement, or the use of drones in agriculture, aiming at higher productivity and increased income for the farmer.

CONCLUSIONS

Total porosity showed a high positive correlation with permanent wilt point. Soil water availability showed a high positive correlation with soil density and a high negative correlation with free porosity. In turn, free porosity showed a high negative correlation with soil density.

In general, all attributes showed spatial dependence, standing out soil density and permanent wilt point, which were the best evaluators of strong spatial dependence.

ACKNOWLEDGMENTS

This study was partially granted by the Coordination for the Improvement of Higher Education Personnel – Brazil (CAPES) – Financial Code 001.

This study was supported by the National Council for Scientific and Technological Development (CNPq) – Brazil (grant number 141231/2019-0).

REFERENCES

- Alencar CAB, Cunha FF, Martins CE, Coser AC, Rocha WSD, Araújo RAS (2009) Irrigação de pastagens: atualidade e recomendações para uso e manejo. *Revista Brasileira de Zootecnia* 38(1): 98-108. DOI: <https://dx.doi.org/10.1590/S1516-35982009001300012>
- Almeida E (2012) *Econometria espacial aplicada*. Campinas, Alínea, 498 p.
- Anselin L, Syabri I, Kho Y (2006) "Geoda: An introduction to spatial data analysis", *Geographical Analysis* 38(1). DOI: <https://dx.doi.org/10.1111/j.0016-7363.2005.00671.x>
- Bernardo S, Mantovani EC, Silva DD, Soares AA (2019) *Manual de irrigação*. Viçosa, UFV, 9 ed. 545p. ISBN:9788572696104
- Bezerra RR, Silva EFF, Siqueira GM, Dantas DC, Almeida BG, Silva AO (2019) Least limiting water range in Spodosol and initial growth of sugarcane under soil bulk densities and salinities. *Revista Brasileira de Engenharia Agrícola e Ambiental* 23(11): 833-839. DOI: <http://dx.doi.org/10.1590/1807-1929/agriambi.v23n11p833-839>
- EMBRAPA - Empresa Brasileira de Pesquisa Agropecuária (2018) *Sistema brasileiro de classificação de solos*. Embrapa, 5 ed rev ampl.
- Martins EL, Silva Souza RF da, Fraga VS, Magalhães AG, Medeiros, SS (2019) Efeitos da variabilidade espacial da densidade do solo e fração grosseira na estimativa dos estoques de nutrientes em solo degradado. *Brazilian Journal of Development* 5(12): 29434-29449. DOI: <https://dx.doi.org/10.34117/bjdv5n12-099>
- Nascimento LFC, Batista GT, Dias NW, Catelani CS, Becker D, Rodrigues L (2007) Análise espacial da mortalidade neonatal no Vale do Paraíba, 1999 a 2001. *Revista Saúde Pública* 41c(1): 94-100. Available: <http://www.scielosp.org/pdf/rsp/v41n1/14.pdf>
- Neves C, Camara MRG da, Sesse Filho UA, Esteves EG Z, Marconato M (2015) Análise do índice de Gini nos municípios de Santa Catarina em 2000 e 2010: uma abordagem exploratória de dados espaciais. *Revista Brasileira de Estudos Regionais e Urbanos* 9 (2) 209-227. Available: <https://revistaaber.org.br/rberu/article/view/145>
- Oliveira JT, Passos M de, Roque CG, Baio FHR, Kamimura KM, Ribeiro IS, Teodoro PE (2018) Space variability of phenological indicators of common bean crop. *Bioscience Journal* 34(2). DOI: <https://dx.doi.org/10.14393/BJ-v34n2a2018-39659>
- Oliveira JT, Oliveira RA de, Oliveira LAA, Teodoro P, Montanari R (2020a) Spatial variability of irrigated garlic (*Allium sativum* L.) Production Components. *HortScience* 55(3): 300-303. DOI: <https://doi.org/10.21273/HORTSCI14409-19>
- Oliveira JT, Oliveira RA de, Puiatti M, Teodoro P, Montanari R (2020b) Spatial analysis and mapping of the effect of irrigation and nitrogen application on lateral shoot growing of garlic. *HortScience* 1: 1-2. DOI: <https://doi.org/10.21273/HORTSCI14881-20>
- Soares M, Campos M, Oliveira I, Cunha J, Souza Z, Aquino R, Silva J (2018) Variabilidade espacial dos atributos do solo sob agroflorestal na região de Humaitá, AM. *Gaia Scientia* 12(1): 33-41.
- Tavanti RF, Montanari R., Panosso AR, Freddi ODS, Paz-González A (2020) Pedotransfer function to estimate the soil structural "S" index and spatial variability in an oxisol within a livestock farming system. *Engenharia Agrícola* 40 (1): 34-44. DOI: <https://dx.doi.org/10.1590/1809-4430-eng.agric.v40n1p34-44/2020>